Measurement of absolute flow velocity vector using dual-angle, delay-encoded Doppler optical coherence tomography

Cameron J. Pedersen

Department of Biomedical Engineering, Case Western Reserve University, Cleveland, Ohio 44106-7207, USA

David Huang

Doheny Eye Institute, University of Southern California, Los Angeles, California 90033, USA

Mark A. Shure

Cole Eye Institute, Cleveland Clinic Foundation, Cleveland, Ohio 44195, USA

Andrew M. Rollins

Departments of Biomedical Engineering and Medicine, Case Western Reserve University, Cleveland, Ohio 44106-7207, USA

Received August 2, 2006; revised October 27, 2006; accepted November 3, 2006;
posted November 20, 2006 (Doc. ID 73739); published February 2, 2007

Single-beam laser Doppler measurements of flow velocity are only sensitive to the velocity component parallel to the optical axis. We describe a simple modification to a standard Doppler optical coherence tomography (OCT) system using a single sample beam that provides velocity information from multiple angles within the beam. By introducing a glass plate midway into the OCT beam path, the sample beam is divided into several components, each with a different group delay and each providing a separate interferogram with its own effective Doppler angle. By combining the Doppler shift measured in each of these component interferograms, the flow velocity vector is fully determined. © 2007 Optical Society of America

OCIS codes: 170.4500, 170.3340, 170.3890.

Optical coherence tomography (OCT) is an emerging imaging modality that provides noncontact, high-resolution structural images of biological tissue.[1,2] Based on principles of low-coherence interferometry, the amplitude of the interferometric signal is used to map varying reflectivity within the sample. Doppler optical coherence tomography (DOCT) is a functional extension of OCT that uses the phase of the OCT signal to detect moving scatterers within tissue.[3,4] It is well known that the optical Doppler effect can be exploited to obtain velocity measurements of moving scatterers within living tissue. However, single-beam laser Doppler measurements of flow velocity are sensitive to only the velocity vector component parallel to the optical axis of the beam. Our target application is DOCT imaging of small vessels within the retina. When the angle of the probe beam with respect to the vessel is not known *a priori*, an absolute measurement of flow velocity in a plane will require single-beam measurements at no less than two different angles (absolute flow in 3D requires at least three angles). Techniques in laser Doppler velocimetry have been developed using beams at multiple angles to determine both the axial and transverse velocity components.[5,6] More recently, techniques in DOCT have been developed to address this problem. The first uses measurements of Doppler frequency shift and Doppler frequency broadening to determine the Doppler angle.[7] However, frequency broadening measurements can measure the total flow speed but not the vector direction in 3D. Moreover, the data suggest a significant increase in measurement uncertainty at slower velocities (i.e., less than 20 mm s^{-1}) and at angles near 90°. Another method employs the use of a quadrant detector in a free-space interferometer to determine the velocity.[8] This technique is not amenable to fiber-based OCT systems. Dave and Milner have developed a technique using DOCT that measures velocity at two different angles and encodes the resultant OCT signals in orthogonal polarization states.[9] In the context of the retina, polarization encoding is vulnerable to cross-talk due to birefringence in the cornea and crystalline lens. In this Letter, we demonstrate a technique, using a single sample beam, that provides velocity information from multiple angles within the beam. By introducing a glass plate into the OCT beam path, the sample beam is divided into two components, each with a different group delay and each probing the sample at a different angle. Because they experience different delays, the signals representing the two probe angles are independently detectable. By making use of the Doppler shift measured in each of these component interferograms, the flow velocity vector is fully determined in the plane of the two component beams. By aligning the plane of these component beams parallel to the length of the blood vessel, we can obtain an absolute measurement of velocity.

As illustrated in Fig. 1(a), to find a flow velocity vector V, one can obtain velocity measurements v_1 and v_2 with a known separation angle between the two measurements of θ by finding the angles of incidence α_1 and α_2, such that

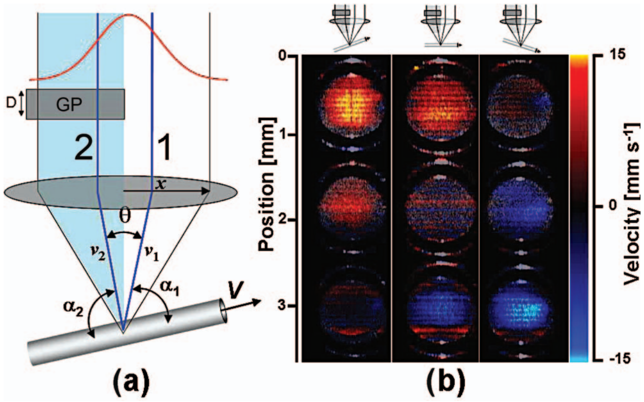

Fig. 1. Dual-angle, delay-encoded DOCT probe beam (a) and resultant flow phantom images (b). The three subimages in each panel are the three delay-encoded signals representing from top to bottom the undelayed path (1+1), the two degenerate singly delayed cross paths (1+2 and 2+1), and the doubly delayed path (2+2). The red curve in (a) denotes the Gaussian profile of the collimated sample beam. The blue lines indicate rays at the effective centers of the two beam components (see text). The horizontal striations in (b) are due to nonlinear motion in the reference arm scanner.

$$\alpha_1 = \tan^{-1}\left(\cot\theta - \frac{v_2}{v_1 \sin\theta}\right),$$

$$\alpha_2 = \pi - \theta - \alpha_1.$$

The magnitude of the velocity vector V is then simply

$$V = \frac{v_1}{\cos\alpha_1} = \frac{v_2}{\cos\alpha_2}.$$

The technique of path-length-encoding components of a single OCT beam was introduced by Iftimia *et al.* for speckle reduction in OCT images.[10] A glass plate of thickness D is placed midway into the collimated OCT sample beam as shown in Fig. 1(a). When the glass plate is inserted into the sample beam, the beam is subdivided into two beamlets, each with different optical delay and each with different angles of incidence on the sample. Assuming scattering as well as specular reflection, incident light rays can travel one of four paths through this optical system as shown in Fig. 1(a). The light may be incident via path 1 and return via either path 1 or path 2. Similarly, the light may be incident via path 2 and return via either path. Since the two "cross" paths experience the same optical delay, they are effectively degenerate and the resultant OCT signal is a set of three images, the degenerate central one and two satellites, each separated by a delay of $D(n-1)/2$ (where D and n are the thickness and refractive index of the glass plate, respectively).

To calculate the effective separation angle θ, we assume that the OCT probe beam is a Gaussian beam converging onto the sample. The beam is described by a Gaussian amplitude profile,

$$A(r) = A_0 e^{-(r/r_0)^2},$$

with a peak field amplitude of A_0 on the optical axis, falling off by a factor of e^{-1} at a radius of r_0. We assume that the glass plate intersects exactly half of the beam. The effective center of the half-beam is given by the amplitude-weighted first moment of the transverse distance x from the center of the beam where the glass plate edge is located, as shown in Fig. 1(a),

$$\bar{x} = \frac{\int_0^{\pi}\int_0^{\infty} xA(r)2\pi r \mathrm{d}r\mathrm{d}\phi}{\int_0^{\pi}\int_0^{\infty} A(r)2\pi r \mathrm{d}r\mathrm{d}\phi} = \frac{\int_0^{\infty} e^{-(r/r_0)^2} r^2 \mathrm{d}r \int_0^{\pi} \sin\phi \mathrm{d}\phi}{\int_0^{\infty} e^{-(r/r_0)^2} r \mathrm{d}r \int_0^{\pi} \mathrm{d}\phi} = \frac{r_0}{\sqrt{\pi}},$$

where r and ϕ are the polar coordinates in the plane normal to the beam and $x \equiv r\sin\phi$. If we consider the beam profile at the location of the lens of focal length f in Fig. 1(a), then the effective angle between the two beamlets is given by

$$\theta = 2\arctan(r_0/f\sqrt{\pi}),$$

where θ is defined in Fig. 1(a). The lines in Fig. 1(a) labeled v_1 and v_2 represent the rays at the effective center of beamlets 1 and 2, respectively.

To demonstrate the feasibility of delay-encoded DOCT, we used a conventional bench-top time-domain OCT imaging system with a broadband light source (1291 nm center wavelength, 21 μm coherence length). For an OCT sample beam with an e^{-2} intensity width (i.e., $2r_0$) of 6.8 mm and an objective lens with a focal length of 30 mm, we calculated our effective separation angle to be 7.3°. For a standard Gullstrand eye,[11] a beam of equivalent numerical aperture (6.8/30) would fit within a pupil of 4.3 mm, which is smaller than the average pupil size in dim light.[12] To verify this angle calculation by measurement, a mirror was first placed in the sample plane. The optical axis of the scanning beam was set normal to the mirror surface, and a 5 mm thick glass plate was placed halfway into the probe beam proximal to the scanning mirrors. The angles at which each satellite peak experienced maximum amplitude were recorded, and the difference was taken to be the effective separation angle. Subsequently, a flow phantom consisting of a 0.6 mm inner diameter glass capillary tube containing flowing 5% Intralipid was placed in the sample beam and tilted on the same apparatus used for the previous experiment. Figure 1(a) shows the orientation of the phantom to the bisected OCT beam. A previously described autocorrelation algorithm was used to estimate velocity.[13,14] The angles at which each satellite Doppler image measured zero flow were recorded and the difference was also taken to be a measurement of the effective separation angle. The phantom was then imaged by scanning

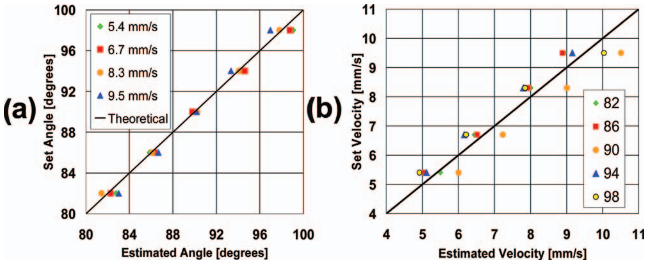

Fig. 2. Estimation of (a) Doppler angle and (b) velocity using the dual-angle, delay encoded technique. Solid line, unity slope.

Table 1. RMS Errors for Estimation of Doppler Angle

	Angle of Incidence				
	82°	84°	90°	94°	98°
RMS error	0.72°	0.38°	0.21°	0.47°	0.84°

Table 2. RMS Errors for Estimation of Velocity for Each Angle of Incidence

	Angle of Incidence				
	82°	84°	90°	94°	98°
RMS error (nm/s)	0.37	0.40	0.73	0.43	0.45

the probe beam perpendicular to the plane shown in Fig. 1(a). These data are shown as three OCT images in Fig. 1(b). In the case of the mirror and the flow phantom, the separation was measured to be 7.4° and 7.5°, respectively, in good agreement with the predicted effective angle.

To investigate the ability of this technique to measure Doppler angle and absolute velocity, the same flow phantom was again placed into the OCT sample beam with the previously described configuration. A 4 by 5 factorial experiment (i.e., 20 images total) was conducted, wherein dual-angle, delay-encoded DOCT images were recorded in random order at four different flow velocities (ranging from 5.4 to 9.5 mm/s) and at five different incidence angles (ranging from 82° to 98°). The satellite velocities were measured for each image and, using the equations given above, estimates of Doppler angle and absolute velocity were calculated. Figure 2(a) shows the angle estimation at the four different flow rates. As can be seen, these estimations are in agreement with the true angle as set with a goniometer on which the sample stage was mounted. The average RMS error of these measurements was 0.52°. These data are summarized in Table 1. Figure 2(b) shows the estimation of absolute average velocity within the flow phantom compared with the true velocity as set by a precision pump. Velocity estimates are shown for each angle of incidence. The average RMS error of the velocity measurements was $0.48\ \mathrm{mm\,s^{-1}}$. These data are summarized in Table 2.

To conclude, we have described a Doppler OCT imaging technique that is capable of measuring absolute velocity of moving scatterers. By introducing a glass plate into the sample beam of an existing OCT system, this method can be used to estimate Doppler angle and absolute velocity. Although this demonstration was performed using a time-domain OCT system, we believe this technique is as easily implemented in a spectral-domain system. However, it should be mentioned that to sufficiently separate the satellite images one must use an increased scan range. Since the retina is relatively thin (~1 mm), a minor sacrifice in resolution could be made to gain the necessary scan range. Although this technique has been demonstrated for two dimensions, we believe it to be sufficient to obtain absolute velocity measurements when used for vessels in the retina since, with the use of a camera to visualize the vasculature, one dimension can be eliminated by orienting the plane containing the beamlets parallel to the axis of the vessel. It also follows that, with the implementation of a more complex optical delay element, three dimensions could be probed.

The authors acknowledge the contributions of Roger Lin and Michael Jenkins. This work was supported by the Whitaker Foundation (RG-02-0376) as well as the National Eye Institute (R01 EY013516). This work was conducted in a facility constructed with support from Research Facilities Improvement Program Grant Number C06 RR12463-01 from the National Center for Research Resources, National Institutes of Health. A. M. Rollins' e-mail address is andrew.rollins@case.edu.

References

1. D. Huang, E. A. Swanson, C. P. Lin, J. S. Schuman, W. G. Stinson, W. Chang, M. R. Hee, T. Flotte, K. Gregory, C. A. Puliafito, and J. G. Fujimoto, Science **254**, 1178 (1991).
2. A. F. Fercher, W. Drexler, C. K. Hitzenberger, and T. Lasser, Rep. Prog. Phys. **66**, 239 (2003).
3. J. A. Izatt, M. D. Kulkarni, S. Yazdanfar, J. K. Barton, and A. J. Welch, Opt. Lett. **22**, 1439 (1997).
4. Z. Chen, T. E. Milner, D. Dave, and J. S. Nelson, Opt. Lett. **22**, 64 (1997).
5. C. Riva, G. T. Feke, B. Eberli, and V. Benary, Appl. Opt. **18**, 2301 (1979).
6. G. T. Feke, D. G. Goger, H. Tagawa, and F. C. Delori, IEEE Trans. Biomed. Eng. **BME-34**, 673 (1987).
7. D. Piao and Q. Zhu, Appl. Opt. **42**, 5158 (2003).
8. A. Royset, T. Storen, F. Stabo-Eeg, and T. Lindmo, in Proc. SPIE 6079, 607925 (2006).
9. D. P. Dave and T. E. Milner, Opt. Lett. **25**, 1523 (2000).
10. N. Iftimia, B. Bouma, and G. J. Tearney, J. Biomed. Opt. **8**, 260 (2003).
11. A. Gullstrand, in *Handbuch der Physiologischen Optik*, 3rd ed., H. von Helmholtz, ed. (Voss, 1909), Appendix II, p. 299.
12. B. Winn, D. Whitaker, D. B. Elliot, and N. J. Phillips, Invest. Ophthalmol. Visual Sci. **35**, 1132 (1994).
13. A. M. Rollins, S. Yazdanfar, J. Barton, and J. Izatt, J. Biomed. Opt. **7**, 123 (2002).
14. A. M. Rollins, S. Yazdanfar, R. Ung-arunyawee, and J. A. Izatt, Proc. SPIE **3598**, 168 (1999).